

Critical magnetic field of disordered Zr-Cu alloys: Density of states and spin-orbit scattering time

A. Nordström and Ö. Rapp

Department of Solid State Physics, The Royal Institute of Technology, S-100 44 Stockholm, Sweden

Z.-Y. Liu*

Department of Physics, Chalmers Institute of Technology, S-412 96 Gothenburg, Sweden

(Received 10 October 1989)

The critical magnetic field H_{c2} is measured for disordered Zr_xCu_{1-x} for $0.36 < x < 0.65$ in magnetic fields up to 3.5 T and temperatures down to 30 mK. Werthamer-Helfand-Hohenberg theory is found to describe the data well. The density of states $N(0)$ and the spin-orbit relaxation time τ_{so} are determined by fitting to the whole critical-field curve. We investigate how accurately these parameters can be obtained from critical-field measurements. τ_{so}^{-1} is found to depend weakly on the Zr ionic mass. It is suggested that accurate critical-field data can give supplementing information in the study of weak localization and interaction effects. Evidence is found for some enhancement of $N(0)$ obtained from the critical field as compared to results from the specific heat, thus confirming an earlier conjecture by Poon. Comparison with several published results suggests that this enhancement is small and only about 5–10 %.

I. INTRODUCTION

The upper critical magnetic field H_{c2} of glassy metallic superconductors has remained controversial in different aspects. For instance, it is not clear whether H_{c2} is anomalously enhanced at low temperatures^{1–3} or not,^{4–6} nor what is the reason for such enhancement. A larger value of H_{c2} than consistent with traditional Werthamer-Helfand-Hohenberg (WHH) theory⁷ may be due to inhomogeneities,^{8–10} even on a length scale below 100 Å, or to a depression in magnetic field¹¹ of a weak-localization-induced enhancement¹² of the Coulomb pseudopotential μ^* . Furthermore, it has been pointed out¹³ that according to the Fukuyama-Ebisawa-Maekawa (FEM) theory,¹⁴ weak localization contributions to H_{c2} may be almost indistinguishable from the WHH theory in the weakly disordered region. A method has been proposed to detect such contributions in glassy metals.¹³

In order to study an enhancement of H_{c2} , one must reach low reduced temperatures $t = T/T_c \approx 0.2$, where these effects, if present, are most pronounced. This condition has not always been fulfilled in the past which may have contributed to some of the controversies quoted. In this paper we report on measurements of the upper critical field of disordered Zr-Cu alloys in the range from 36 to 65 at. % Zr. These alloys have zero-field T_c values below 2 K, allowing us to reach $t < 0.1$ at moderate field strengths, < 3.5 T, in a dilution refrigerator for most of the samples.

Within such a series of weakly disordered alloys one expects at most small variations of disorder. Therefore, if H_{c2} is enhanced, there is a possibility to separate effects from weak localization and inhomogeneities in a similar way as reported previously for disordered Nb-Ni alloys.³ It is found however that H_{c2} of Zr-Cu alloys is generally well described by WHH theory. We investigate how ac-

curately the spin-orbit scattering time τ_{so} and the density of states, $N(0)$, can be obtained from H_{c2} , and compare our results with published values from the normal state magnetoresistance and specific heat experiments. In particular, we discuss if the critical field results for $N(0)$ are enhanced over those obtained from the specific heat.

II. EXPERIMENTAL DETAILS AND RESULTS

Alloys were prepared by arc-melting appropriate amounts of Zr (nominal purity 99.9 wt. %) and Cu (99.95 wt. %). Amorphous samples were produced by melt spinning onto a rapidly revolving copper wheel in a vacuum chamber filled with argon gas. The cross section of the ribbons was typically $30 \mu\text{m} \times 1.5 \text{ mm}$.

In experiments on metallic glasses there is a possibility that structural differences between different samples of similar chemical composition will affect the results. Therefore we also investigated two samples, $Zr_{50}Cu_{50}(1)$ and $Zr_{65}Cu_{35}$, prepared about 10 years ago from elements of nominal purities of at least 99.99 wt. %. These samples were characterized previously¹⁵ and have since been stored in air at room temperature. The equiatomic sample made presently by us is denoted $Zr_{50}Cu_{50}(2)$.

Both sides of the samples were subjected to x-ray analysis at room temperature (Ni-filtered Cu $K\alpha$ radiation) and were found to be x-ray amorphous. The resistance of the samples was measured with a standard four-probe dc technique and low current densities, $< 0.5 \text{ A/cm}^2$. The transitions in magnetic field were studied by sweeping the field at constant temperatures with low sweep rates of about 1.3 T/h. Thus eddy current heating could be avoided even at the lowest temperatures. In the region 1.5–2.0 K the measurements of H_{c2} were performed in a pumped He bath between the poles of an electromagnet, with the field perpendicular to the sample current. The homogeneity of this magnet is better than

10^{-4} . The temperature was obtained from a calibrated carbon resistor and from the vapor pressure of the He bath. Below 1.5 K the measurements were performed in a dilution refrigerator equipped with a superconducting solenoid, which provided a magnetic field oriented parallel to the sample current, with a homogeneity of 10^{-2} . The temperature was measured with a calibrated carbon resistor.

In order to check the quality of our samples we characterized them in several ways. The superconducting transition temperature in zero magnetic field, defined as the temperature where the resistivity is 50% of its value at 4.2 K, is shown in the lower part of Fig. 1, together with results from the literature. The position of the first peak in the structure factor k_p is shown in the top part of Fig. 1. Our results for T_c and k_p are well within the range of values typical for metallic glasses from different sources.

The superconducting transition widths were defined in zero field as the temperature interval where the resistivity changes from 10% to 90% of its value at 4.2 K. In magnetic field the widths were defined as the field interval corresponding to the same change of the resistivity. The widths in zero field were in the range from 5 mK ($Zr_{36}Cu_{64}$) to 32 mK ($Zr_{60}Cu_{40}$) with typical values around 20 mK. In magnetic field typical widths were 80 mT at $t=0.6$ and 100 mT at $t=0.1$, with an exception for $Zr_{36}Cu_{64}$ where the widths were 15 mT at $t=0.6$ and 20 mT at $t=0.3$.

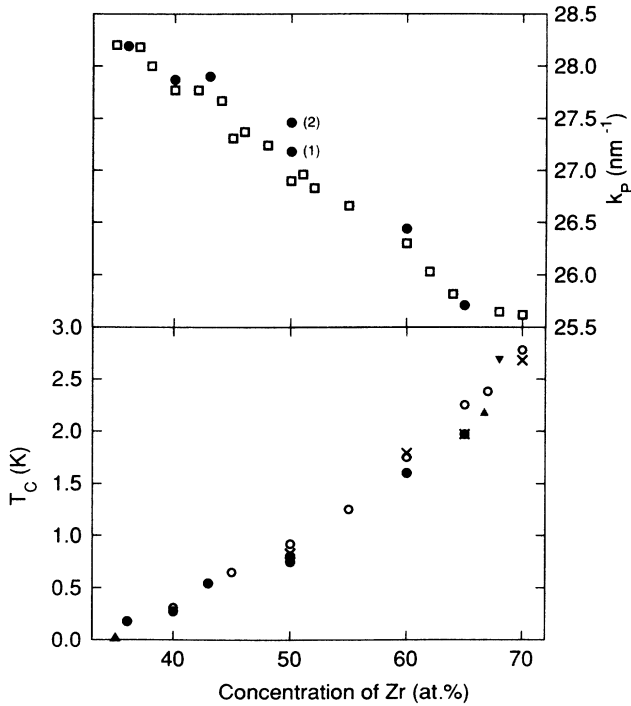


FIG. 1. Results for Zr-Cu metallic glasses. Top: First peak in structure factor k_p ($=4\pi \sin\theta/\lambda$). \square : Ref. 16, \bullet : present results. (1) and (2) denote the two $Zr_{50}Cu_{50}$ alloys from different sources described in the text. Bottom: Superconducting transition temperature \times : Ref. 17; \blacktriangle : Ref. 18; \triangle : Ref. 19; \circ : Ref. 20; ∇ Ref. 21; \bullet : present work.

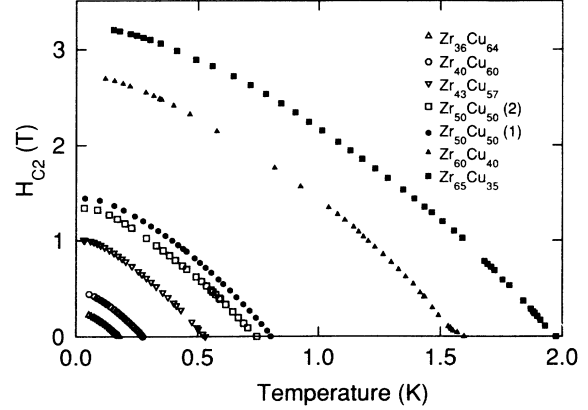


FIG. 2. Upper critical field of glassy Zr-Cu alloys.

The two samples $Zr_{50}Cu_{50}(1)$ and $Zr_{65}Cu_{35}$ which had been stored for an extended time, did not show any relaxation effects. The samples had retained their shiny metallic surfaces. The transition temperatures were the same and the transition widths similar to the results of the previous measurements.^{15,18}

The results for H_{c2} are shown in Fig. 2. We reach $t < 0.1$ for all samples except $Zr_{40}Cu_{60}$ ($t_{\min} = 0.19$) and $Zr_{36}Cu_{64}$ ($t_{\min} = 0.28$). The change of experimental equipment at about 1.5 K is barely visible in the data. When measurements are performed close to $t = 1$, one can sometimes observe a small region of anomalous curvature of either sign,^{3,8,10,17} such as for $Zr_{60}Cu_{40}$ in Fig. 2. This effect is not well understood. It somewhat increases the error in the parameters determined in the fitting procedures.

III. ANALYSIS AND RESULTS OF FITTING PROCEDURES

A. WHH theory

The WHH theory gives a solution to the linearized Gor'kov equations for H_{c2} of a bulk weakly coupled type-II superconductor, including effects of Pauli spin paramagnetism and spin-orbit scattering.⁷ In the dirty limit (i.e., short electron mean free path), which is applicable for amorphous metals, one obtains $H_{c2}(t)$ as the magnetic field B which satisfies

$$\ln \frac{1}{t} = \left[\frac{1}{2} + \frac{i\lambda_{so}}{4\gamma} \right] \Psi \left[\frac{1}{2} + \frac{\bar{h} + \frac{1}{2}\lambda_{so} + i\gamma}{2t} \right] + \left[\frac{1}{2} - \frac{i\lambda_{so}}{4\gamma} \right] \Psi \left[\frac{1}{2} + \frac{\bar{h} + \frac{1}{2}\lambda_{so} - i\gamma}{2t} \right] - \Psi \left[\frac{1}{2} \right] \quad (1)$$

at $t = T/T_c$. Ψ is the digamma function, $\gamma \equiv [(\alpha\bar{h})^2 - (\frac{1}{2}\lambda_{so})^2]^{1/2}$, $\bar{h} = eBD/k_B\pi T_c$, D is the electronic diffusivity, λ_{so} the spin-orbit interaction parameter, and α the Maki paramagnetic limitation parameter.²²

α can be calculated either from the normal state resistivity and the normal state electron specific heat, or from the slope of the critical field curve at T_c . In the latter case

$$\alpha = -0.528 \left[\frac{dH_{c2}}{dT} \right]_{T=T_c} \quad (2)$$

with H_{c2} in Tesla.

When fitting the theory to experimental data it is convenient to use a reduced critical field $h^* = \bar{h} / (-d\bar{h}/dt)_{t=1} = \pi^2 \bar{h} / 4$, which can be calculated from experimental results by

$$h^* = - \frac{H_{c2}(T)}{T_c (dH_{c2}/dT)_{T=T_c}} \quad (3)$$

B. Fitting procedures

Critical-field data are often analyzed by fitting a straight line to the region close to T_c , which gives α from Eq. (2). As has been pointed out⁶ such a procedure always underestimates α .

Following Ref. 6 we have regarded both α and λ_{s0} as adjustable parameters and searched for the combination of these parameters which gives the lowest root-mean-square value (rms) calculated from all data points for each sample. For each tested value of α we computed $h^*(t)$ and $\bar{h}(t)$ from Eqs. (2) and (3). α and λ_{s0} were varied in a grid net, and for each point in this net, the rms value of a fit to Eq. (1) was calculated. We get good fits of the WHH theory. Figure 3 shows an example of such a fit. For one sample, $Zr_{43}Cu_{57}$, the renormalized H_{c2} coincides with the WHH maximum curve.

It is of interest to determine how accurately α and λ_{s0} can be obtained from the critical field. This uncertainty was estimated in the following way. First we calculated the area in the α - λ_{s0} plane where the rms value of the fit is equal to or less than twice the smallest rms value. An example is shown in Fig. 4 for the same sample as in Fig. 3.

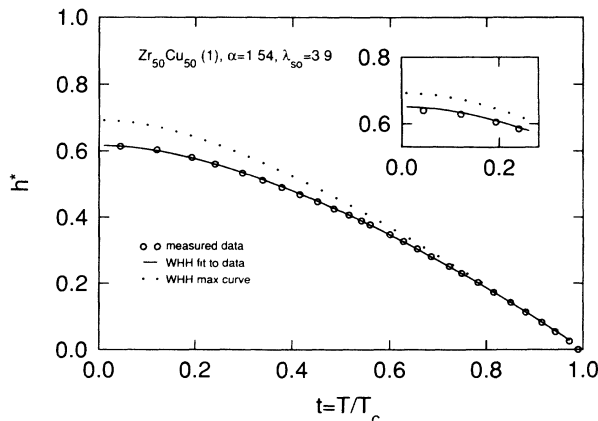


FIG. 3. Example of a fit to the WHH theory with parameters given in the figure. Insert: low t -region of a fit with α and λ_{s0} at one end point of the area shown in Fig. 4.

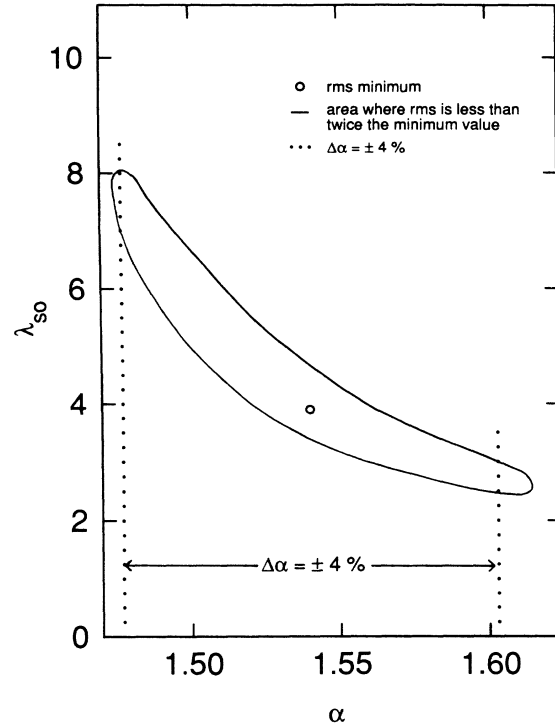


FIG. 4. Illustration for $Zr_{50}Cu_{50}(1)$ how confidence intervals for α and λ_{s0} are obtained. The vertical lines represent the maximum variation of α as determined from Fig. 5.

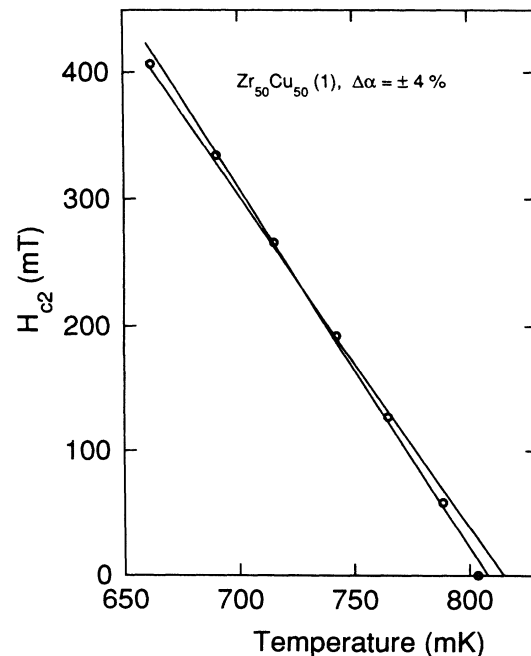


FIG. 5. H_{c2} close to T_c for $Zr_{50}Cu_{50}(1)$. The two straight lines show the extremal values of the critical field slope that are consistent with experimental data.

TABLE I. Results for disordered Zr-Cu alloys.

Sample	α	$\pm\Delta\alpha(\%)$	λ_{so}	$\Delta\lambda_{so}$	$h^*(0)$	rms(10^{-3})
Zr ₃₆ Cu ₆₄	1.22	2.8	3.0	1.9–6.2	0.631	2.33
Zr ₄₀ Cu ₆₀	1.41	7.9	6.0	2.1–>100	0.645	3.82
Zr ₄₃ Cu ₅₇	1.44	0.9	∞	—	0.693	<2.10
Zr ₅₀ Cu ₅₀ (1)	1.54	4.1	3.9	2.5–7.6	0.617	2.42
Zr ₅₀ Cu ₅₀ (2)	1.45	1.5	8.6	6.2–13.1	0.655	4.70
Zr ₆₀ Cu ₄₀	1.55	8.4	1.87	1.1–4.4	0.573	4.67
Zr ₆₅ Cu ₃₅	1.46	4.0	2.0	1.4–3.1	0.586	2.71

For a few samples the rms minimum is rather shallow which makes the plotted area more extended, especially toward high λ_{so} values since the WHH theory is insensitive to large changes of λ_{so} in this region. Taking twice the minimum rms value as an estimate of the error is a rather conservative measure which clearly affects the quality of the fit. This is illustrated in the insert of Fig. 3 which shows the low- t region of a fit to the experimental data with parameters at one extremal point of the region displayed in Fig. 4.

Equation (2) provides a second method to investigate the uncertainty in α . Straight lines were fitted to the data in the region $0.8 \leq t \leq 1.0$. Figure 5 illustrates two extremes, obtained by allowing the rms value of the fits to reach twice the minimal value. For the sample in Fig. 5 this implies a variation of the slope within $\pm 4\%$. It can be seen that these lines are at the limit of being consistent with experimental data. The corresponding range of variation of α values is shown in Fig. 4. We estimate the errors in α and λ_{so} to be well restricted to the intersection of these two areas.

The results for α and λ_{so} and their estimated errors are shown in Table I. The values obtained for $h^*(0)$ and the rms deviation in the best fit are also given. In the WHH theory one always has $h^*(0) \leq 0.693$.

C. The density of states

In order to compare the density of states with results from other experiments without having to rely on estimates of the electron-phonon coupling λ , we calculate the unrenormalized $N(0)$ from⁷

$$N(0) = -\frac{\pi}{4k_B L} \frac{M}{\rho d} \left(\frac{dH_{c2}}{dt} \right)_{t=1}, \quad (4)$$

L is Avogadro's number, d the mass density, M the molecular weight, and ρ the normal state resistivity. For the densities and the resistivities we have used least square fits to our own and published data,^{19,20,23} which minimizes the errors in d and ρ . These errors are below 2%. ρ and d in Eq. (4) should be evaluated in the normal state close to T_c . $\rho(4.2)$ is larger than $\rho(290)$ by several percent and we correct for this difference, while the differences in densities are expected to be smaller by an order of magnitude and are neglected. The results are shown in Fig. 6. An error estimate is indicated for a representative point.

The results from Poon's analysis¹³ of the critical field

data of Samwer and v. Löhneysen¹⁷ below 70 at. % Zr are shown in Fig. 6. For larger Zr concentration, minute crystallites can distort measurements of the resistivity in otherwise amorphous samples. This may be the case, e.g., for Zr₇₄Cu₂₆ in Fig. 1 of Ref. 17, where the temperature coefficient of resistance deviates from the trend of the other alloys in contrast to the linear relation between λ and $d\rho/dT$ expected for disordered Zr-based alloys.²⁴ Therefore the critical field datum for this alloy has been omitted in Fig. 6. Specific heat on the other hand measures a bulk property and the different open symbols show all results from several sources.^{17,25–27}

Disregarding for the moment the straight lines in Fig. 6, the results are in agreement at the level of about 10% in $N(0)$. This remains valid also when results²⁰ from the critical field slope close to T_c are included, and reinforces the conclusion that at this level the simpler method to evaluate $N(0)$ is adequate and that consistent results are obtained from the specific heat and critical magnetic field.²⁸ Since in Sec. IV below we want to investigate the possibility of small systematic differences between specific heat and critical field results for $N(0)$, results evaluated from the critical field slope have been omitted in Fig. 6.

It can be noted that this agreement between different

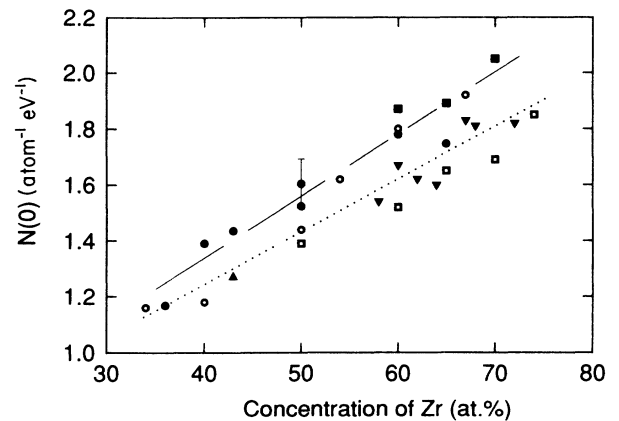


FIG. 6. Density of states for Zr-Cu alloys. Open symbols: from specific heat; filled symbols: from H_{c2} using the whole critical field curve. \square : Ref. 17; \triangle : Ref. 25; \circ : Ref. 26; ∇ : Ref. 27; \blacksquare : Ref. 13; \bullet : present work. An error bar of about 6% is shown for Zr₅₀Cu₅₀(1). Two linear least square fits are shown; dotted line: specific heat data only; dashed line: critical field data only. Note that the unrenormalized $N(0)$ is plotted, which thus contains a factor $(1 + \lambda)$.

results for $N(0)$ apparently breaks down for highly disordered sputtered Zr-Cu alloys,²¹ where the results from the critical field slope are similar to the trend in Fig. 6 but the specific heat results are much larger and may include some additional disorder contribution.

D. The spin-orbit scattering time

From λ_{so} we can determine the spin-orbit scattering time τ_{so} by

$$\tau_{so}^{-1} = 3\pi k_B T_c \lambda_{so} / \hbar. \quad (5)$$

The results are shown in Fig. 7. The error in these results is much larger than for α ; a factor of 2 uncertainty would generally be expected. There is good agreement however, between our data and those of Poon¹³ at 60 and 65 at. % Zr, which supports the consistency of the two analyses and suggests that the small differences in $N(0)$ between Poon's results and ours in Fig. 6 may be due to errors in the resistivity.

Alternatively, τ_{so} can be obtained from the normal state magnetoresistance of disordered metals. The presence of superconducting fluctuations adds further complications to these analyses. We have found two such results for τ_{so} of disordered Cu-Zr alloys, both for $Zr_{43}Cu_{57}$, one²⁹ from the temperature range from 1.2 to 15 K in fields up to 6 T, the other³⁰ from 4.2 K and 30 T. In the latter case fluctuations are expected to be effectively quenched, and this result should be more reliable. Nevertheless the two estimates agree well as shown in Fig. 7. Also in magnetoresistance it is difficult to determine τ_{so} within a factor of 2 or more. Examples were given recently for Cu-Ti alloys.³¹ Therefore the agreement between magnetoresistance and critical-field results in Fig. 7 is quite satisfactory and suggests the possibility to obtain supplementing information from accurate critical-field data in the study of weak localization and interaction effects.

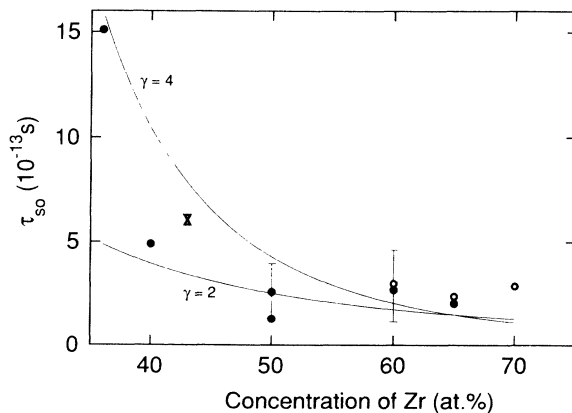


FIG. 7. Spin-orbit scattering time for Zr-Cu alloys. ∇ : from magnetoresistance, Ref. 29; \triangle : from magnetoresistance, Ref. 30; \circ : from critical field, Ref. 13; \bullet : present work. Error bars are shown for two representative points. The two curves illustrate $\tau_{so}^{-1} \sim M_{Zr}^{\gamma}$.

The spin-orbit scattering rate τ_{so}^{-1} increases with atomic mass. The electrons at the Fermi surface of disordered Zr-Cu alloys are predominantly of Zr- d character.³² We simply assume $\tau_{so}^{-1} \sim M_{Zr}^{\gamma}$, where M_{Zr} is the Zr ionic mass. This concentration dependence is shown in Fig. 7 for $\gamma=2$ and 4. The data are consistent with the general form of such a mass dependence. It is not possible to determine an exponent from the present experiments, but we can conclude that it is likely to fall in the range 2–4, which is significantly smaller than values in the range 8–12, sometimes suggested.³³

IV. DISCUSSION OF ENHANCEMENT EFFECTS

A. $h^*(0)$

The WHH theory can be fitted to our critical field data with reasonable values of τ_{so} except for $Zr_{43}Cu_{57}$. As mentioned, the maximum WHH curve fits the data for this sample, corresponding to infinite spin-orbit scattering rate. This result is not understood. Inhomogeneities are a less likely explanation since the superconducting transition widths are small for all of the present samples, and the width for $Zr_{43}Cu_{57}$ is even below the average of the other samples. From an investigation of several glassy alloy systems,⁶ a trend was found for increased values of $h^*(0)$ with increasing atomic number. This can clearly not be applied to a series of alloys in one alloy system such as in Table I, where in contrast there is a weak trend of a decrease of $h^*(0)$ with average atomic number. It was found that $h^*(t=0.3)$ increased with resistivity for a number of amorphous superconductors¹ and the same trend was found in glassy Nb-Ni alloys,³ where $h^*(0) > 0.693$, and interpreted in terms of a weak localization effect. This observation is possibly related to a high value of $h^*(0)$ for $Zr_{43}Cu_{57}$ since ρ is large here. It cannot explain the results in detail because the maximum in ρ as a function of Zr concentration actually occurs at a somewhat smaller concentration. Obviously the question why H_{c2} is enhanced in some alloys and not in others deserves further attention.

B. $N(0)$

It can be seen from Fig. 6 that the critical-field data for the density of states at the Fermi level $N_{H_{c2}}(0)$ are not randomly scattered in the specific heat data $N_c(0)$, but tend to lie in the region of larger values of $N(0)$. We assume that $N(0)$ is linear in concentration and analyze this difference by fitting straight lines separately to the $N_{H_{c2}}(0)$ and $N_c(0)$ data. These two lines are shown in Fig. 6. The scatter of the data around the two lines are similar with rms values somewhat above and below $0.08(\text{atom}^{-1}\text{eV}^{-1})$ for $N_c(0)$ and $N_{H_{c2}}(0)$, respectively, corresponding to 4–6 % of $N(0)$. The difference between the two straight lines is somewhat larger. We conclude that there is some evidence for a small enhancement of order 5–10 % of $N(0)$ obtained from the critical field as compared to results from the specific heat.

Strong-coupling corrections would not seem to be

relevant for the present alloys. Rainer and Bergmann³⁴ calculated a correction factor to Eq. (4) for several typical electron-phonon spectra and for amorphous metals this factor was within 1 ± 0.05 . Wong *et al.*⁶ considered strong-coupling corrections to critical-field parameters in an intuitive way and found them to be small. In addition, the present alloys are rather weak or medium-coupled superconductors. Even for a small disorder induced enhancement of μ^* to a value³⁵ of 0.15, one is in the region $\lambda < 0.6$ for all of the present alloys, where any strong-coupling corrections would be less important.

Weak localization contributions were considered by Poon¹³ in a calculation from the FEM theory.¹⁴ An enhancement factor $\{[N_{H_{c2}}(0)/N_c(0)] - 1\}$ was calculated as a function of $E_F\tau/\hbar$. Here E_F is the Fermi energy and τ the (elastic) relaxation time. According to this calculation an enhancement of 5–10% corresponds to $E_F\tau/\hbar$ in the range 3–4. In a free electron model $E_F\tau/\hbar = [(3\pi^2)^{2/3}\hbar]/(2e^2n^{1/3}\rho)$ with n the number density of carriers. For n in the range¹⁸ $(5-9) \times 10^{28} \text{ m}^{-3}$ and $\rho = 170 \mu\Omega \text{ cm}$ one obtains values for $E_F\tau/\hbar$ between 2.5 and 3.1. Considering the rough nature of this calculation the agreement with the model is fair.

Our enhancement is smaller than 15–20%, as obtained by Poon.¹³ Such differences may be due to some difficulty in the analysis, such as finding correct values for ρ , or possibly to systematic differences between samples from different sources. Our analysis is based on average properties of samples from several sources. The $N_{H_{c2}}(0)$ results in Fig. 6 are obtained from three different sources and the $N_c(0)$ results from one of these and three other sources. This gives some confidence in an enhanced

$N_{H_{c2}}(0)$ as a general average property of Zr-Cu metallic glasses.

V. CONCLUDING REMARKS

Summarizing, we have shown that for disordered Zr-Cu alloys, results for $N(0)$ at the level of about 5% and for τ_{so} within a factor of 2 can be obtained from measurements of the critical field over an extended temperature range down to below about $t=0.2$. By comparison with several results from specific heat measurements, a small enhancement of $N(0)$ from H_{c2} can be inferred, of order 5–10% in qualitative agreement with predictions from FEM theory.

It is not known how τ_{so} is affected when small corrections from the FEM theory in the weakly localized regime are included in the WHH theory. However, the agreement in Fig. 7 between results for τ_{so} from magnetoresistance and critical field suggests that at the level of accuracy illustrated in the figure, τ_{so} is not influenced by possible FEM corrections. Critical-magnetic-field measurements would thus seem to be a useful supplement to the study of weak localization and interaction effects by magnetoresistance.

ACKNOWLEDGMENTS

We are grateful to P. Lindqvist for discussions and stimulation at the early stages of this work and to Ch. Torpling for his help with the dilution refrigerator. One of us (Z.-Y.L.) is thankful to T. Claeson and his group at Chalmers for their hospitality. This project was supported by the Swedish Natural Science Research Council and the Swedish Board for Technical Development.

*Present address: Institute of Physics, Academy of Science, P.O. Box 603, Beijing, China.

¹M. Tenhover, W. L. Johnson, and C. C. Tsuei, *Solid State Commun.* **38**, 53 (1981).

²M. Ikebe, Y. Muto, S. Ikeda, H. Fujimori, and S. Suzuki, *Physica* **107B**, 387 (1981).

³Ö. Rapp and P. Lindqvist, *Phys. Lett. A* **120**, 251 (1987).

⁴W. Eschner and W. Gey, in *Superconductivity in d- and f-Band Metals—1982*, edited by W. Buckel and W. Klose (Kernforschungszentrum, Karlsruhe, FRD, 1982), p. 359.

⁵M. G. Karkut and R. R. Hake, *Phys. Rev. B* **28**, 1396 (1983).

⁶K. M. Wong, E. J. Cotts, and S. J. Poon, *Phys. Rev. B* **30**, 1253 (1984).

⁷N. R. Werthamer, E. Helfand, and P. C. Hohenberg, *Phys. Rev.* **147**, 295 (1966).

⁸W. L. Carter, S. J. Poon, G. W. Hull, and T. H. Geballe, *Solid State Commun.* **39**, 41 (1981).

⁹G. E. Zwicknagl and J. W. Wilkins, *Phys. Rev. Lett.* **53**, 1276 (1984).

¹⁰H. Adrian, N. Toyota, B. Hensel, and K. Söldner, *Jpn. J. Appl. Phys.* **26** (Suppl. 26-3), 1309 (1987).

¹¹L. Coffey, K. A. Muttalib, and K. Levin, *Phys. Rev. Lett.* **52**, 783 (1984).

¹²P. W. Anderson, K. A. Muttalib, and K. V. Ramakrishnan,

Phys. Rev. B **28**, 117 (1983).

¹³S. J. Poon, *Phys. Rev. B* **31**, 7442 (1985).

¹⁴H. Fukuyama, H. Ebisawa, and S. Maekawa, *J. Phys. Soc. Jpn.* **53**, 1919 (1984); **53**, 3560 (1984).

¹⁵Ö. Rapp, B. Lindberg, H. S. Chen, and K. V. Rao, *J. Less Common Metals* **62**, 221 (1978).

¹⁶K. H. J. Buschow, *J. Phys. F* **14**, 593 (1984).

¹⁷K. Samwer and H. v. Löhneysen, *Phys. Rev. B* **26**, 107 (1982).

¹⁸Ö. Rapp, J. Jäckle, and K. Froböse, *J. Phys. F* **11**, 2359 (1981).

¹⁹E. Babic, R. Ristic, M. Miljak, and M. G. Scott, in *Proceedings of the 4th International Conference on Rapidly Quenched Metals*, Sendai, 1981, edited by T. Masumoto and K. Suzuki (Inst. of Metals, Sendai, 1982), p. 1079.

²⁰Z. Altounian and J. O. Strom-Olsen, *Phys. Rev. B* **27**, 4149 (1983).

²¹O. Laborde, J. C. Lasjaunias, F. Zougmore, and O. Bethoux, *Z. Phys. Chem.* **157**, 743 (1988).

²²K. Maki, *Physics* **1**, 127 (1964).

²³D. Pavuna, *J. Non-Cryst. Solids* **61-62**, 1353 (1984).

²⁴M. Flodin, L. Hedman, and Ö. Rapp, *Phys. Rev. B* **34**, 4558 (1986).

²⁵D. E. Moody and T. K. Ng, *Inst. Phys. Conf. Proc.* **55**, 631 (1981).

²⁶P. Garoche and J. Bigot, *Phys. Rev. B* **28**, 6886 (1983).

- ²⁷J. Tebbe and K. Samwer, *Z. Phys. B* **63**, 163 (1986).
- ²⁸C. C. Koch, D. M. Kroeger, J. O. Scarbrough, and B. C. Giessen, *Phys. Rev. B* **22**, 5213 (1980).
- ²⁹J. B. Bieri, A. Fert, G. Creuzet, and J. C. Ousset, *J. Appl. Phys.* **55**, 1948 (1984).
- ³⁰J. C. Ousset, H. Rakoto, J. M. Broto, and S. Askenazy, *Solid State Commun.* **56**, 291 (1985).
- ³¹P. Lindqvist and G. Fritsch, *Phys. Rev. B* **40**, 5792 (1989).
- ³²P. Oelhafen, E. Hauser, H. J. Guntherodt, and K. H. Benneman, *Phys. Rev. Lett.* **43**, 1134 (1978).
- ³³B. J. Hickey, D. Grieg, and M. A. Howson, *J. Phys. F* **16**, L13 (1986).
- ³⁴D. Rainer and G. Bergmann, *J. Low Temp. Phys.* **14**, 501 (1974).
- ³⁵Ö. Rapp, *Phys. Rev. B* **34**, 2878 (1986).